



UNIVERSITY OF LEEDS

This is a repository copy of *Dye-Mediated Interactions in Chitosan-Based Polyelectrolyte/Organoclay Hybrids for Enhanced Adsorption of Industrial Dyes*.

White Rose Research Online URL for this paper:
<http://eprints.whiterose.ac.uk/143134/>

Version: Accepted Version

Article:

Huang, P, Xia, D, Kazlauciusas, A orcid.org/0000-0002-5859-0811 et al. (3 more authors) (2019) Dye-Mediated Interactions in Chitosan-Based Polyelectrolyte/Organoclay Hybrids for Enhanced Adsorption of Industrial Dyes. *ACS Applied Materials & Interfaces*, 11 (12). pp. 11961-11969. ISSN 1944-8244

<https://doi.org/10.1021/acsami.9b01648>

© 2019 American Chemical Society. This is an author produced version of a paper published in *ACS Applied Materials & Interfaces*. Uploaded in accordance with the publisher's self-archiving policy.

Reuse

Items deposited in White Rose Research Online are protected by copyright, with all rights reserved unless indicated otherwise. They may be downloaded and/or printed for private study, or other acts as permitted by national copyright laws. The publisher or other rights holders may allow further reproduction and re-use of the full text version. This is indicated by the licence information on the White Rose Research Online record for the item.

Takedown

If you consider content in White Rose Research Online to be in breach of UK law, please notify us by emailing eprints@whiterose.ac.uk including the URL of the record and the reason for the withdrawal request.



eprints@whiterose.ac.uk
<https://eprints.whiterose.ac.uk/>

Dye-mediated Interactions in Chitosan-based Polyelectrolyte/Organo-clay Hybrids for Enhanced Adsorption of Industrial Dyes

Peng Huang^{*†}, Dong Xia[†], Algy Kazlauciusas[†], Paul Thornton[†], Long Lin[†] and Robert Menzel^{*†}

[†]School of Chemistry, University of Leeds, Leeds, LS2 9JT, U.K.

Non-covalent, dye-mediated interactions between organo-montmorillonites (“organo-clays”) and a chitosan-based polyelectrolyte are exploited for highly effective and fast removal of different, industrially-important anionic dyes (single-azo, double-azo, anthraquinone) from aqueous solutions. The addition of only 10 wt% of polyelectrolyte to a conventional organo-clay results in a 100% increase in absolute dye uptake capacity, an acceleration of dye uptake kinetics by up to 500%, and the flocculation of large, easily-separable sorbent aggregates. These substantial improvements in adsorption performance are driven by the mediating effect of the anionic dyes (acting as electrostatic mediator between the positively-charged polyelectrolyte chains and organo-clays), enabling the formation of true hybrid sorbent structures without the need for covalent crosslinking chemistry. The dye-mediated sorption and hybrid formation mechanism is further evidenced by structural and chemical characterization of the hybrid sorbents (small angle XRD, IR mapping) as well as by analysis of dye sorption kinetics according to the intraparticle diffusion model. Importantly, the organo-clay/polyelectrolyte hybrid system provides a highly interesting adsorbent for the treatment of dye mixtures. Our study shows that structurally different anionic dyes localise at different sites within the hybrid structure (organo-clay intergallery spaces vs polyelectrolyte/organo-clay interface), enabling the simultaneous adsorption of different dyes with high efficiency. Consequently, the total uptake capacity for dye mixtures was 50% larger than that of individual dyes, demonstrating the enormous potential of the hybrids for industrial wastewater purification, where dye mixtures are ubiquitous.

KEYWORDS: organic/inorganic hybrids, water treatment, adsorption, dye mixtures, biopolymers, montmorillonite, intraparticle diffusion, flocculation

INTRODUCTION

Discarded textile dyes have become a major source of water pollution¹, as a result of the development of the textile industry. Some 40 billion tons of water are used in the textile industry each year to produce the required amounts of fabrics². The resulting dyeing effluent alone accounts for 17%-20% of global water pollution². Reactive anionic dyes comprise one of the major classes of dyes used industrially³, of which C.I. Reactive Black 5 is the most extensively used. In general, during the current dyeing process, only a maximum of 70%-80% of the reactive dye becomes fixed to cellulosic fibers, the rest being washed off into the effluent in the form of hydrolyzed dye⁴. Issues arise when the colored wastewater is discharged to the watercourse and river basins⁵. The presence of unnatural colors in surface water is aesthetically unpleasant and causes disturbance and harm to the aquatic biosphere⁶. In some instances, the closure of dyehouses and of dye-producing factories has been inevitable. Therefore, appropriate treatment technologies need to be developed to address the effluent problem⁷.

Effective, fast dye removal is essential prior to effluent discharge⁸. Among the conventional dye-effluent treatment techniques, adsorption to a solid substrate is one of the more economical and viable methods^{9, 10}. Characteristics include excellent affinity towards target dye molecules, high adsorption capacities and the possibility of adsorbent regeneration influence

the selection of adsorbents employed¹¹. Typically, dye removal efficiency is affected by physical factors and by chemical factors¹² such as dye-adsorbent interactions, the particle size and the surface area of the adsorbent, solution pH, temperature and the dye-substrate contact time⁵.

Montmorillonite (MMT) is considered to be a highly-promising, economically-viable adsorbent¹³, due to its abundance in nature, its large surface area and the ease of its modification. MMT, a subclass of smectite, is an expanding 2:1 layered clay, consisting of two tetrahedral sheets of silica that sandwich a central alumina octahedral sheet. Natural MMT usually exhibits relatively poor affinity for anionic dyes due to the like surface charges of the two substances; therefore, modifications are necessary to furnish the clays with enhanced anionic dye adsorption capacities¹⁴. The compensating cations on the surface of the MMT layers can be exchanged with other polar or ionic organic compounds, leading to the formation of organo-montmorillonites (organo-clays). As a result, the modification of montmorillonite, using organic compounds, has been widely explored in a variety of applications¹⁵⁻¹⁷. However, the adsorption of dyes onto organo-clays is relatively slow, and it remains a key challenge to enhance the dye adsorption rate and the uptake capacity of the organo-clays, simultaneously. Cationic polyelectrolytes enable effective and highly efficient precipitation of anionic species from bulk solution¹⁸, owing to their outstanding chelation capability. Consequently, it is particularly interesting, and potentially highly beneficial, to incorporate polyelectrolytes into organo-clays to produce materials that are exceptional candidates for the comprehensive treatment of dyehouse effluents.

Electronic Supplementary Information (ESI) available: [details of any supplementary information available should be included here]. See DOI: 10.1039/x0xx00000x

ARTICLE

Chitosan (CTS) is a linear polysaccharide that is composed of β -(1-4)-linked *D*-glucosamine (deacetylated unit) and *N*-acetyl-*D*-glucosamine (acetylated unit), produced by the deacetylation of chitin, the second most-abundant natural polysaccharide in the world¹⁹. CTS possesses a number of intrinsic characteristics that make it promising as an environmentally friendly biosorbent for color removal: (1) the low cost compared to activated carbon²⁰, (2) the outstanding chelation capacities for a wide-range of target dyes, and (3) the ability to be supported on solid materials²⁰. To improve the chemical stability and adsorption capacity, modifications are essential if the CTS is to possess specific characteristics, such as the molecular weight, the crystallinity and the degree of deacetylation, and the stability²¹. The most commonly adopted chemical modifications to introduce different functional groups are cross-linking²², grafting *via* functional groups^{23, 24}, carboxymethylation²⁵ and acetylation²¹. Despite good adsorption performances having been reported for chitosan derivatives, prominent problems associated with such materials are the low porosity and surface area, which hamper their rate of dye adsorption. Moreover, crosslinking that is typically used to improve the stability and recoverability of the chitosan-based materials may significantly deteriorate the dye uptake capacity and adsorption rate²⁰. In principle, these drawbacks can be overcome by using a water-soluble chitosan derivative as a polyelectrolyte, which would result in immediate dye capture from aqueous solutions. Combining a chitosan-based polyelectrolyte with organically modified MMT, exploits the advantageous features of both materials and is thus highly-attractive for deployment as a versatile dye adsorbent.

Herein, we report an effective and highly efficient route for the treatment of dyehouse effluents by combining cationic polyelectrolyte N-[(2-hydroxy-3-trimethylammonium)propyl] chitosan chloride (HTCC) with surfactant-modified clays (Fig 1), without the requirement of chemical crosslinking. The chemical modification of chitosan improves charge density for industrial dye removal at very basic pH conditions. Three widely used anionic industrial dyes, Reactive Black 5, Reactive Blue 19 and Reactive Red 195 were chosen as the model target dyes. Importantly, these dyes have been hydrolyzed to simulate real-life dyeing effluents which contain reactive dyes in their hydrolyzed form. A series of physicochemical measurements, including liquid-phase adsorption capacities, kinetics and thermodynamics, on the adsorption of various hydrolyzed dyes have been carefully designed to provide quantitative data which are pertinent to understanding the adsorption mechanism.

EXPERIMENTAL SECTION

Materials

Chitosan [$>75\%$ deacetylation degree, having a viscosity of 800–2000 mPa s for a solution of 1 wt% of chitosan in 1% acetic acid in water (25 °C, Brookfield)] having a molecular formula of $(C_8H_{13}NO_5)_n$ was supplied by Sigma-Aldrich (UK). Sodium-montmorillonite, a pale brown powder having a cation exchange

capacity of 85.3 mmol/100 g and an average particle size of 7 μ m, was purchased from Alfa Aesar (UK). Isopropyl alcohol $[(CH_3)_2CHOH]$, A.R. Grade] and cetyltrimethylammonium bromide ($C_{19}H_{42}BrN$, CTAB) were obtained from Fisher Scientific (UK). 2,3-Epoxypropyltrimethylammonium chloride ($C_6H_{14}NOCl$, EPTAC) and sodium hydroxide were purchased from Sigma-Aldrich (UK). Commercial grade Reactive Black 5, Reactive Blue 19 and Reactive Red 195, widely used anionic dyes in industry, with claimed purities of 88%, 68% and 95%, respectively, were obtained from Regency FCB Ltd. (UK).

Preparation of polyelectrolyte (HTCC) and organo-clay (OMMT)

The HTCC samples were prepared based on a modification of the method proposed by Zhao *et al.*²⁶. Pre-dried CTS (5 g) was dissolved in 450 mL of 2% acetic acid in aqueous solution. Then, an aqueous solution of sodium hydroxide (4 M) was added dropwise until the pH reached 9. The CTS precipitate was washed repeatedly with deionized water until neutral. Then, the product was filtered and freeze-dried for further use. The product was obtained at 84% yield. 2 g of the freeze-dried CTS was dispersed in a mixture of isopropanol/water (20 mL/16 mL), at 35 °C, over 30 minutes. The temperature was set to 60 °C, and 5.65 g of EPTAC, in aqueous solution (35wt%), were added. The mixture was heated under reflux, at 60 °C, for 6 h to form N-[(2-hydroxy-3-trimethylammonium)propyl] chitosan chloride (HTCC). Finally, the product was washed with acetone, filtered, dried under vacuum at 50 °C and stored for subsequent experiments.

Details concerning the preparation of organically modified montmorillonite (OMMT) can be found elsewhere²⁷. In this study, an organic modifier (here CTAB) loading fraction of three times the cation exchange capacity of pristine sodium-montmorillonite was selected as it has been reported to be optimal for hydrolyzed dye removal.

Batch dye adsorption experiments

To mimic real dyehouse effluents, dye hydrolysis was performed under thermal (80 °C) and alkaline conditions (pH = 12) for 1 hour²⁸ and all experiments were carried out using the hydrolyzed form of the industrial dye. Prior to dye adsorption, OMMT was dispersed in deionized water (1 wt%) and then mixed with a known volume of an aqueous HTCC stock solution (1 wt%), in order to vary the HTCC:OMMT ratio. Unless otherwise stated, adsorption experiments were carried out at pH 7 and 20 °C, using 100 mL aqueous dye solution at an initial dye concentration of 100 mg/L and at an adsorbent loading of 80 mg/100 mL. After stirring for 26 h, equilibrium was reached for all dyes and the residual dye concentration in solution determined *via* UV-vis spectroscopy at the maximum absorption wavelength (see ESI for calibration equations). For the kinetic studies, aliquots of the dye solutions were extracted at pre-determined time intervals and the absorbance value determined following the same experimental procedure. To explore the adsorption thermodynamics, dye uptake was measured at four different

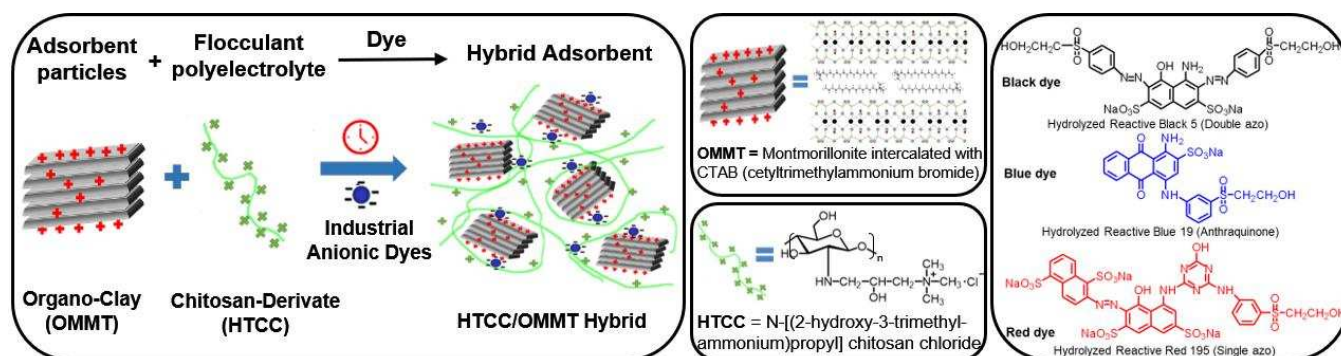


Figure 1 Schematic representation of anionic dye removal by cationic polyelectrolyte (HTCC)/organo-clay (OMMT) hybrid adsorbent.

temperatures (20, 30, 40, 50 °C), using an initial dye concentration of 150 mg/L. In order to investigate the competitive dye adsorption, experiments were carried out using a dye mixture (hydrolyzed Reactive Blue 19 and hydrolyzed Reactive Red 195, each with an initial concentration of 100 mg/L). The absorbance value of the blue dye in the mixture was determined at a wavelength of 632 nm (where the red dye has no absorption). The absorbance value of the red dye in the mixture was calculated from the absorbance at 543 nm, by subtracting the absorbance value of the blue dye at the same wavelength. The concentrations of the blue dye and the red dye were determined using the corresponding calibration equations (ESI).

Various adsorption kinetic models were employed to investigate the adsorption behavior of the hydrolyzed dyes. The pseudo-second-order kinetic model assumes that chemisorption is the rate controlling parameter and is expressed as²⁹:

$$\frac{t}{q_t} = \frac{1}{q_e} t + \frac{1}{k_2 q_e^2}$$

Here, q_t is the amount of adsorbed dye at time t , q_e is the amount of adsorbed dye at equilibrium, and k_2 is the rate constant for the pseudo-second-order kinetic model.

The intraparticle diffusion kinetic model describes the diffusion of the dye molecules from the bulk solution onto the porous adsorbent particles³⁰:

$$q_t = k_i t^{1/2} + C$$

Here, q_t is the amount of adsorbed dye at time t , k_i is the rate constant for the intraparticle diffusion model, and C is the intercept of the regression curve.

The half-adsorption time is defined as the time required for the adsorbent to reach half of the equilibrium adsorption capacity, and is expressed as follows³¹:

$$t_{1/2} = \frac{1}{k_2 q_e}$$

The thermodynamic parameters related to the adsorption process (adsorption enthalpy, ΔH° , and adsorption entropy, ΔS°) are calculated as follows³²:

$$\log \frac{q_e m}{C_e} = \frac{\Delta S^\circ}{2.303R} + \frac{-\Delta H^\circ}{2.303RT}$$

Here, q_e is the amount of adsorbed dye at equilibrium, C_e is the equilibrium dye concentration in solution, m is the amount of adsorbent used in the aqueous solution ($\text{g}\cdot\text{L}^{-1}$); and T is the absolute

temperature. The ratio of q_e/C_e is usually used to express the adsorption affinity³³.

Materials characterization

Small-angle X-ray diffraction (XRD) patterns were measured, using a Bruker D8 Advance X-ray diffraction equipment. The tests were performed from 1.5° to 15° with a step size 0.026°, using Cu K α radiation ($\lambda = 0.154$ nm), at a generator voltage of 40 kV and a current of 40 mA. The d -spacing of the clay layers was calculated according to Bragg's law. Particle size analysis was conducted using a Malvern Mastersizer 2000 particle size analyzer (Malvern Instruments Ltd., UK). A particle refractive index of 1.5 was assigned to the measurements. The dielectric constant was set at 78.5, and the viscosity was 0.89 mPa S. IR mapping analyses were performed using a PerkinElmer spectrum spotlight FTIR imaging system, in reflection mode.

RESULTS AND DISCUSSION

Dye adsorption characteristics of HTCC/OMMT hybrids

In order to optimize adsorbent composition, the polyelectrolyte (HTCC) percentage in the hybrid adsorbent was systematically increased (relative to the organo-clay (OMMT) amount) and the equilibrium uptake of black dye (hydrolyzed Reactive Black 5) was measured at a fixed total adsorbent loading (80 mg/100 mL). On increasing the relative amount of HTCC in the hybrid, dye uptake initially increased to a maximum of 96% at an optimum adsorbent composition of 10 wt% HTCC and 90 wt% OMMT. The equilibrium uptake capacity of the hybrid for the black dye was 109 mg/g, 190% larger than previously reported results on the removal of the same dye (hydrolyzed Reactive Black 5) using activated sludge³⁴. Interestingly, increasing the relative HTCC content further resulted in sharp decrease in dye uptake (Figure 2a).

Dye adsorption experiments, using the pure HTCC and the pure OMMT components, respectively, were carried out (Figure 2b) to understand this trend and to assess the contribution of the individual components to the total capacity of the hybrid. For the pure organo-clay, dye removal monotonously increased with increased organo-clay loading, due to a straightforward increase in available adsorption sites. Previous structural investigations²⁷ showed that dye adsorption onto OMMT is driven by both electrostatic and partition mechanisms, i.e. by both electrostatic and hydrophobic interactions. With pure organo-clays alone, extremely large adsorbent loadings (176 mg/100

ARTICLE

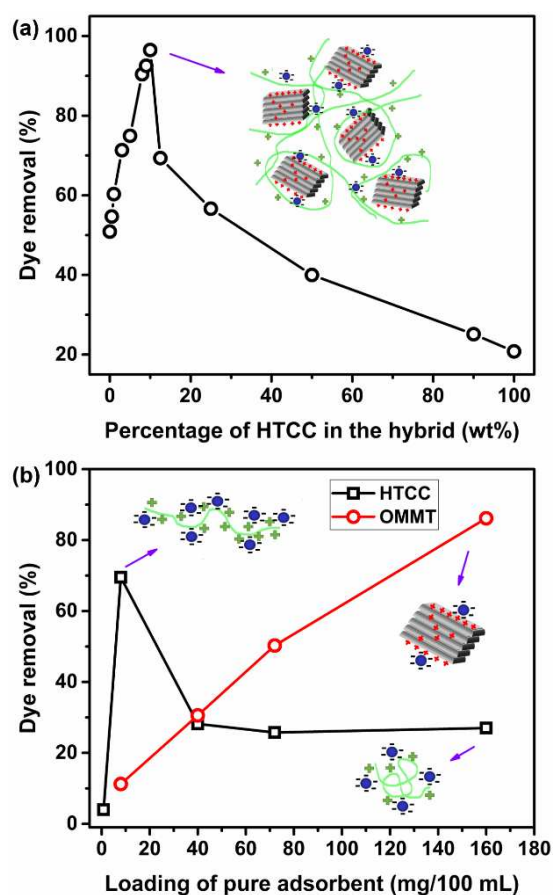


Figure 2 Removal of hydrolyzed Reactive Black 5 from aqueous solutions (pH 7, 20 °C, dye concentration of 100 mg/L, stirred for 26 hours), (a) by HTCC/OMMT hybrids with increasing percentage of HTCC (constant total HTCC/OMMT loading of 80mg/100mL); (b) by pure HTCC and by pure OMMT.

mL) are required to achieve industrially-relevant dye removal efficiencies (>95%), with the associated production of large amounts of waste sludge and the subsequent sludge disposal causing substantial processing issues and environmental concerns. In contrast, using the optimized hybrid adsorbent (10wt% HTCC, 90wt% OMMT) enables high dye removal (96%) at less than half total adsorbent loadings, reducing environmental impact and commercial costs of the effluent treatment process.

Interestingly, the pure polyelectrolyte exhibited a very different adsorption profile compared to the organo-clay. For pure HTCC, dye removal initially increased to a maximum, and then decreased rapidly before levelling off (Figure 2b), mirroring the trend observed for the hybrid adsorbent (Figure 2a). At low HTCC concentration, electrostatic repulsion of the positive charges along the polymer backbone leads to a stretching out of the polymer chain, thereby providing excellent accessibility to the binding sites. However, at higher HTCC concentrations, charge screening effects^{18, 35 36} lead to the collapse of the polymer chains, dramatically reducing the concentration of accessible dye binding sites. Consequently, pure HTCC reaches its dye removal maximum (70%) at a loading equivalent to 10%. However, the very high dye removal of the HTCC/OMMT hybrid (96%) cannot be achieved using HTCC alone. By combining the polyelectrolyte and the organo-clay at an optimized weight ratio, the limitation of each pure material can be overcome,

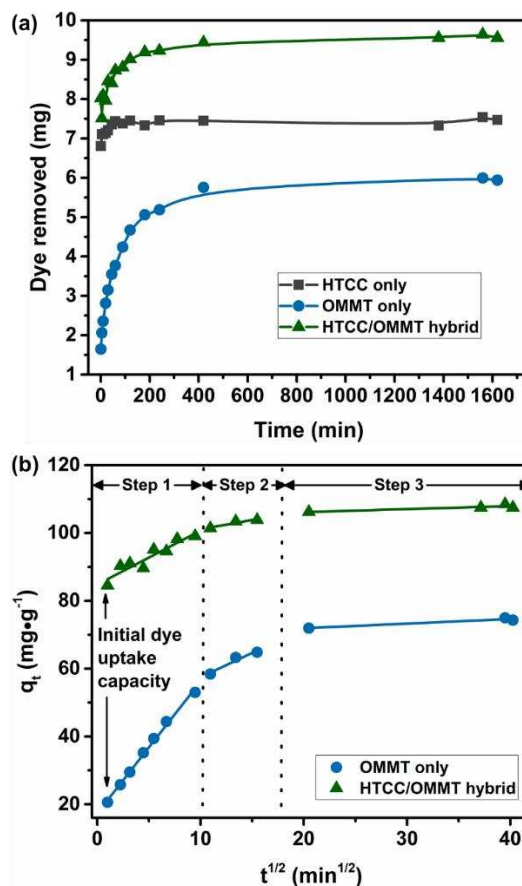


Figure 3 Sorption kinetics for the adsorption of hydrolyzed Reactive Black 5 from aqueous solutions onto pure and hybrid adsorbents (pH 7, 20 °C, dye concentration of 100 mg/L) (a) Dye uptake over time; (b) Intraparticle diffusion model fitting.

Table 1 Dye removal characteristics of the pure and hybrid adsorbents for the aqueous Reactive Black 5 dye solution (100 mg/L, pH 7, 20 °C).

Samples	Dye removal (%)	Initial dye uptake (mg)	$t_{1/2}$ (min)
HTCC	76	6.8	0.9
OMMT	54	1.6	26.2
HTCC/OMMT hybrid	97	7.5	5.4

whilst maintaining high dye uptake capacity at a relatively low loading of adsorbents (Figure 2a).

Kinetic dye adsorption studies were performed for the pure HTCC and OMMT components as well as for the optimized HTCC/OMMT hybrid to gain deeper insight into the mechanism of the adsorption process. The kinetic raw data for pure and hybrid adsorbents (Figure 3a) fitted best to a pseudo-second-order kinetic model, indicating that chemisorption is the rate-controlling parameter in all cases (see ESI). A fast dye adsorption rate is economically important. For the pure organo-clay (OMMT in Figure 3a), comparatively slow dye adsorption was observed, reaching equilibrium after 26 h with an uptake capacity of 76 mg/g. The initial dye uptake (i.e. uptake within one minute) by pure OMMT was only 22 mg/g, further evidencing slow sorption kinetics. However, introducing only 10 wt% HTCC into the system (HTCC/OMMT hybrid in Figure 3a) the sorption kinetics dramatically increased, with an increase of initial dye uptake by 370%, even surpassing the initial uptake capacity of the pure polyelectrolyte (HTCC in Figure 3a). Another practically important

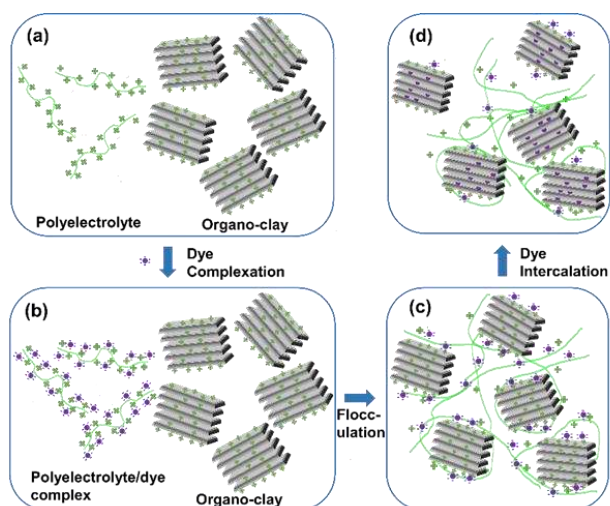


Figure 4 Dye-mediated flocculation and sorption in the HTCC/OMMT hybrid system, (a) HTCC/OMMT hybrid; (b) Dye complexation; (c) Flocculation; (d) Dye intercalation.

measure for the rate of dye adsorption is the half-adsorption time, $t_{1/2}$, defined as the time required for the adsorbent to reach half of the equilibrium adsorption capacity. By incorporating polyelectrolyte into the system, $t_{1/2}$ can be shortened by a factor of 5 compared to the organo-clay (Table 1), with a 43% increase in equilibrium dye uptake capacity. These results further confirm that the adsorption efficiency and uptake capacity of traditional clay adsorbents can be significantly improved by incorporating a small amount of polyelectrolyte.

Analysis of the kinetic data according to the intraparticle diffusion model can provide additional insights into the interactions between dyes and sorbents (Figure 3b). As expected, the kinetic data of the pure polyelectrolyte do not obey the intraparticle diffusion model (see ESI) as no particle-based adsorbents are involved. However, for the pure OMMT and the HTCC/OMMT hybrid systems, three distinct adsorption steps can be distinguished: Step 1) boundary layer diffusion: the initial diffusion of the dye molecules from the bulk solution through the boundary layer onto the external surface of the organo-clay; Step 2) interlamellar diffusion: transport of the dye molecules from the particle surface into the internal clay particle pores and interlamellar spaces; Step 3) adsorption equilibrium: the reaching of adsorption equilibrium in the interlamellar spaces. In Figure 3b, the difference in the Step 1 gradients suggests significantly slower dye diffusion onto the organo-clay surface in the mixed HTCC/OMMT system (compared to pure organo-clay), suggesting an initial, fast formation of larger dye/polyelectrolyte complexes in solution, that then diffuse more slowly through the boundary layer in Step 1. Similar results have been observed for molecular adsorption onto activated carbon, in which smaller molecules exhibited steeper gradient in the boundary layer diffusion step³⁷. Interestingly, the HTCC/OMMT system also shows a significantly larger initial dye removal value compared to the pure OMMT (Table 1), further suggesting that the dye molecules initially bind preferentially to the polyelectrolyte in solution before diffusing to the particle surface (Figure 4b). Having reached the particle surface, the smaller Step 2 gradient of the HTCC/OMMT system implies competing interactions of the dye with polyelectrolyte and organo-clay, resulting in a slower diffusion of the dye molecules into the interlamellar space compared to the pure OMMT system (Figure 4d).

These observations suggest a dye-mediated adsorption and flocculation mechanism for the HTCC/OMMT system (Figure 4). Initial, fast dye binding by the polyelectrolyte in solution ('Dye Complexation', Figure 4b) enables dye-mediated binding of the polyelectrolyte chains onto the positively-charged organoclay particles ('Flocculation', Figure 4c), followed by (partial) diffusion of dye into the clay interlamellar spaces ('Dye Intercalation', Figure 4d). The formation of dye-mediated HTCC/OMMT hybrids was also supported by changes in suspension stability and surface charge upon dye addition. Without the dye, the HTCC/OMMT system was a stable particle suspension and showed a strongly positive zeta potential value (+24.1 mV). However, upon addition of anionic dye, the particle surface charge was significantly reduced (+8.4 mV) and the precipitation of large aggregates was observed (see also Figure 6), further evidencing the mediating effect of anionic dyes in the polyelectrolyte/organo-clay system.

Sorption of different anionic dyes onto HTCC/OMMT hybrids

In order to demonstrate the application of the HTCC/OMMT hybrid systems beyond Reactive Black 5, the adsorption of two additional, industrial anionic dyes (hydrolyzed Reactive Blue 19 (anthraquinone dye), hydrolyzed Reactive Red 195 (single azo dye), Figure 1) was studied. Optimization experiments showed that these two dyes also showed maximum uptake for a polyelectrolyte/organo-clay composition of 10wt% HTCC and 90wt% OMMT (ESI). For all dyes, the hybrid adsorbent exhibited a very high degree of dye removal (>91%) compared to the pure polyelectrolyte and pure organo-clay adsorbents (Table 2). The uptake kinetics for all dyes fitted a pseudo-second-order model (ESI, Figure S9), indicating chemisorption. A slightly lower uptake capacity was detected for the adsorption of hydrolyzed Reactive Red 195 (96 mg/g); however, this value was 100% larger compared to using pure organo-clay.

When expressed in molar units (mmol/g, Table 3) the equilibrium dye uptake capacity for the blue dye is almost double than that of the red and black dyes (Table 3), implying that the HTCC/OMMT hybrid system has a particularly pronounced adsorption affinity for Reactive Blue 19. The particularly high affinity for the blue dye is further indicated by a considerably shorter half-adsorption time (Table 3). For all three dyes, dye removal kinetics fitted well with the intraparticle diffusion model (Figure 5a). In all cases, dye diffusion and adsorption onto particle surface (Step 1) was faster than dye intercalation and intergallery adsorption (Steps 2 and 3, see ESI for numerical values of Step gradients), indicating that diffusion into the interlamellar clay spaces is the rate limiting step. For all three dyes, relatively large initial uptake capacities are observed (69-97 mg/g, Figure 5a), indicating a fast initial dye removal process, likely related to HTCC/dye complex formation (see also discussion above). The largest initial uptake capacity was observed for the blue dye, indicating a particularly pronounced affinity between Reactive Blue 19 and HTCC. In the intraparticle diffusion model (Figure 5a), blue dye adsorption is associated with a very small Step 2 gradient (close to zero), suggesting minimal intercalation of the blue dye, probably due to strong binding of the blue dye to the HTCC polyelectrolyte at the clay surface. In contrast, Reactive Red 195 showed a considerably

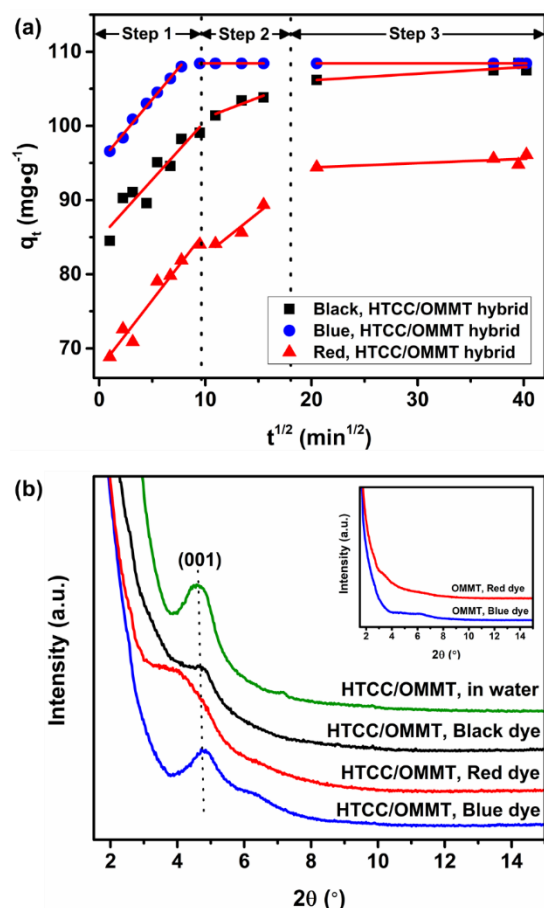


Figure 5 Dye removal characteristics of different dyes from aqueous solutions using HTCC/OMMT hybrid, at pH 7 and 20 °C (a) Intraparticle diffusion kinetic model fitting; (b) Small-angle XRD patterns, before (green trace) and after (black, red and blue trace) dye adsorption. Inset: small-angle XRD patterns of OMMT dyed with blue dye and red dye.

Table 2 Dye adsorption capacities for different dyes using HTCC/OMMT hybrid (80mg/100mL), pure HTCC (8mg/100mL) and pure OMMT (72mg/100mL)

	HTCC/OMMT Hybrid	Pure HTCC	Pure OMMT
Black dye (%)	96	21	51
Blue dye (%)	100	38	86
Red dye (%)	91	15	41

Table 3 Comparison of dye removal characteristics for different dyes onto HTCC/OMMT hybrid.

Samples	q_e		Dye removal (%)	$t_{1/2}$ (min)	d_{001} (nm)
	q_e (mg·g ⁻¹)	q_e (mmol·g ⁻¹)			
Black dye	109	0.14	97	5.44	1.90
Blue dye	109	0.21	100	0.43	1.84
Red dye	96	0.09	87	9.06	2.42

weaker HTCC affinity (e.g. smaller initial uptake capacity) and therefore migrated more readily from the external clay surface into the intergallery clay spaces, as reflected by the steep Step 2 gradient for the red dye adsorption in Figure 5a. These differences in affinity are likely linked to the differences in molecular dye structure (e.g. number and spatial distribution of positive charges and hydrogen bonding groups per dye molecule, Figure 1 and ESI). For example, the red dye bears four anionic sulphonic groups, ideal to maximize interactions with the organo-cations in the organo-clay galleries. In contrast, the blue dye has only one anionic group, but in close proximity to a

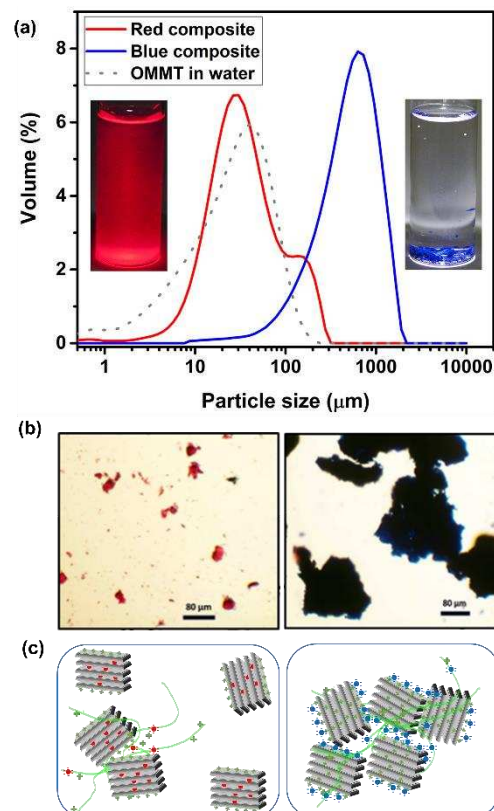


Figure 6 Aggregation of dyed HTCC/OMMT hybrid (a) as determined by laser diffraction measurements; (b) optical micrographs (scale bar 80 μm); (c) schematic representation of red-dyed and blue-dyed HTCC/OMMT aggregates.

hydrogen donor moiety, likely facilitating the interaction and arrangement of Reactive Blue 19 along the HTCC polyelectrolyte chain.

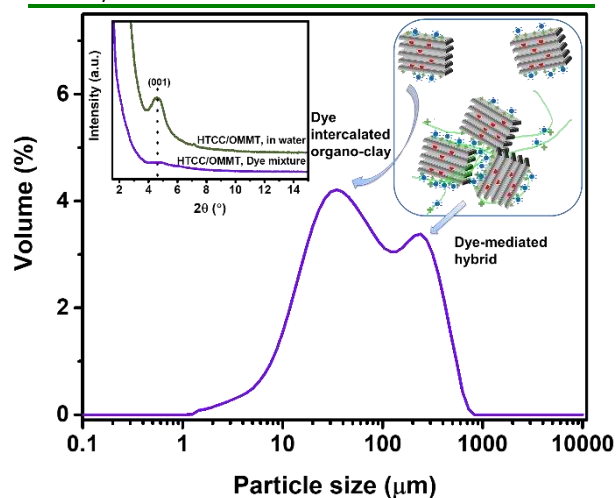
The differences in dye affinity are further corroborated by the aggregation behavior of the hybrid adsorbent particles during the dye removal process. During adsorption of the blue dye, the formation of large particle clusters (average size 640 μm, Figure 6a) is observed, in line with particle bridging through the dye/HTCC polyelectrolyte complexes at the external clay surfaces (Figure 5a). In contrast, for the red dye, much smaller particles (average 55 μm, close to the size of the pure OMMT particle, Figure 6) are observed, indicating the absence of dye-mediated particle bridging and therefore indirectly implying location of the red dye molecules in the particle interior.

In order to confirm that the blue dye is surface-bound, whereas the red dye is intercalated, the interlayer spacings, d_{001} , of the HTCC/OMMT hybrid, both before and after dye adsorption, were determined by small-angle XRD (Figure 5b). The original hybrid showed a broad peak at $2\theta = 4.58^\circ$, corresponding to an interlayer spacing, d -spacing, of 1.93 nm. The peak position of the hybrid remained the same after adsorption of the blue dye (Table 3), confirming that no intercalation occurs. In contrast, the peaks of the hybrid significantly broadened and shifted to lower diffraction angles after adsorption of the red dye, confirming intercalation of the red dye into intergallery clay spaces (Figure 5b).

To understand the nature and energetic changes of dye adsorption onto the HTCC/OMMT hybrid, thermodynamic

Table 4 Comparison of thermodynamic parameters for the adsorption of different dyes onto HTCC/OMMT hybrid (293.15 K)

	ΔG° (kJ mol ⁻¹)	ΔH° (kJ mol ⁻¹)	ΔS° (J mol ⁻¹ K ⁻¹)
Black dye	-3.3	-9.4	-20.9
Blue dye	-6.9	-13.6	-23
Red dye	-1.6	-12.3	-36.6

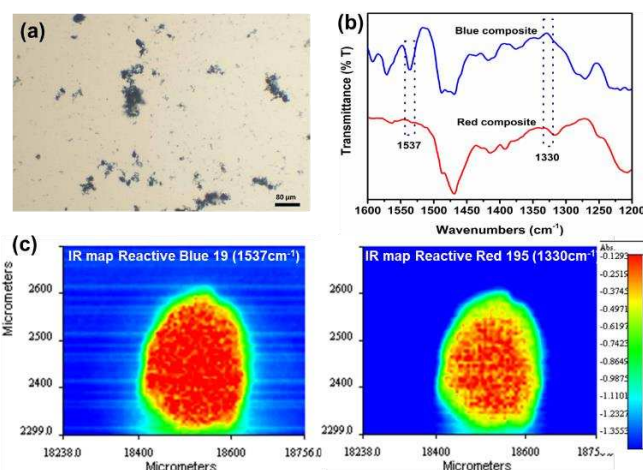
**Figure 7** Aggregation of dye mixture (HTCC/OMMT dyed by 1:1 mixture of the red and blue dyes, 100 mg/L each) as determined by laser diffraction measurements. Inset: (left) Small-angle XRD patterns; (right) Schematic representation of equilibrium dye localisation within the HTCC/OMMT microstructure. Reactive Blue 19 and Reactive Red 195 occupy external and internal adsorption sites, respectively.

parameters, including Gibbs free energy (ΔG°), entropy (ΔS°) and enthalpy (ΔH°), were determined *via* dye adsorption measurements at different temperatures (Table 4). The adsorption of the three dyes onto the HTCC/OMMT hybrid system all showed negative ΔH° and ΔG° values, confirming the exothermic and spontaneous nature of the adsorption process. The more negative absolute ΔG° values for the blue dye (Table 4) implies a more spontaneous adsorption process than for the black and red dyes, and is in line with the high uptake capacities and fast adsorption half-time for the blue dye (Table 3). Adsorption enthalpies (ΔH°) are similar for the three dyes, except a slightly larger absolute value for the blue dye. A relatively large entropic penalty (ΔS°) was observed for the red dye, in line with a reduced degree of freedom of intercalated dye molecules located in the confined interlamellar clay spaces.

Interestingly, thermodynamic, kinetic and structural data all clearly suggest that blue dye and red dye localise at different sites within the HTCC/OMMT hybrid adsorbent (Figure 6c). While the blue dye remains mainly surface-bound due to strong dye-polyelectrolyte interactions, the red dye readily migrates from the external surface and intercalates due to the strong affinity of the red dye for the intergallery spaces (Figure 6c).

Competitive dye adsorption from dye mixtures

In order to test this hypothesis further, we investigated competitive adsorption of mixtures of red dye and blue dye. The study of dye mixtures is also an important, but rarely investigated practical issue in industrial dyeing effluents. Experiments were carried out by batch experiments of the standard HTCC/OMMT

**Figure 8** Adsorption of dye mixture (HTCC/OMMT dyed by 1:1 mixture of the red and blue dye): (a) optical micrograph of dyed HTCC/OMMT particles; (b) IR spectra of Reactive Blue 19 and Reactive Red 195; (c) IR maps of dyed OMMT/HTCC aggregates at 1537 cm⁻¹ (blue dye mapping) and at 1330 cm⁻¹ (red dye mapping).

adsorbent system (10wt%:90wt%) in dye mixture of Reactive Blue 19 (100 mg/L) and Reactive Red 195 (100 mg/L). The bimodal particle size distribution curve indicated the formation of dye intercalated organo-clays (same particle size as OMMT) and dye-mediated hybrids (Figure 7). Optical micrographs suggested the presence of the blue dye for both large and small particles (Figure 8a), while small-angle XRD analysis confirmed the intercalation of the red dye in the organo-clay intergallery space (Figure 7, inset). In order to confirm that blue dye and red dye co-locate within the same adsorbent particle, especially for the dye-mediated hybrid (relatively large-sized particles, Figure 7), the dyed adsorbents were recovered, and IR mapping was performed on individual adsorbent particles, using IR wavelengths exclusively characteristic for Reactive Blue 19 and Reactive Red 195, respectively (Figure 8b). While the spatial resolution of the IR equipment was not sufficient to distinguish the nanoscale location of the red and blue dyes within the organo-clay microstructure, IR maps confirmed that both dyes were present in the same HTCC/OMMT particle and that the adsorption of one dye does not block accessibility for the other dye. The batch adsorption experiments also showed that the total dye uptake in the dye mixture was more than 50% larger compared to the uptake of the individual dyes.

More generally, our results show that combining polyelectrolytes with organo-clay adsorbents (without the need of additional crosslinking chemistry) is an efficient and straightforward strategy to enhance the adsorption performance of traditional particulate clay adsorbents, opening a route for fast and efficient treatment for complex dye mixtures that will be encountered in real-life industrial dyeing effluents.

CONCLUSIONS

A cationic chitosan-based polyelectrolyte has been prepared and used as an efficient, performance-enhancing additive for a conventional cationic organo-clay adsorbent, for the effective treatment of dyeing effluents. The hybrid of

ARTICLE

polyelectrolyte/organo-clay, produced in the absence of covalent crosslinking at a weight ratio of 10/90, showed up to nearly 100% removal of different hydrolyzed anionic dyes, thus exhibiting real potential for use in industry, where dye mixtures are normally encountered in commercial dyeing practices. At this optimized ratio, the cationic polyelectrolyte molecules were fully stretched out and more effective in binding with the anionic dyes. The hybrid exhibited 370% improvement in initial dye uptake capacity and five times faster adsorption rate compared to the organo-clay, as evidenced by the adsorption kinetics. Intraparticle diffusion kinetic model fitting indicated that the hydrolyzed dye molecules were initially bound with the polyelectrolyte to form a complex, then the large complex diffused onto the external surface of the organo-clay. The blue dye was exclusively adsorbed on the external surface and formed large particles due to strong affinity of the polyelectrolyte for the blue dye, whereas the black dye and the red dye could intercalate into the interlamellar space of the clay particles. In particular, dyes with different molecular structures can be adsorbed at different locations without blocking each other, thus the dye uptake capacity for the mixture even exceeds individual dye uptake. Further improvements in the hybrid performance could potentially be achieved by selecting chitosan with higher molecular weight or functionalizing chitosan with more unconventional modifiers (such as cationic moieties with different chain lengths or alternative functional groups). The principles outlined here demonstrate how the adsorption performances of traditional adsorbents can be enhanced through polyelectrolyte addition (without the need for additional covalent crosslinking treatments), for industrial applications where fast adsorption rates, high uptake capacities and separation of spent adsorbent through simple gravitational sedimentation are desirable. More generally, the paper highlights the utility of synergistic interactions between polyelectrolytes and the clays, mediated by small, charged molecules, with wider implications to other polymer-clay application fields, such as pesticide adsorbents, viscosifiers, gas-barrier materials, or mechanically reinforced thermoplastics.

ASSOCIATED CONTENT

Supporting Information

Structure of OMMT, calibration graphs for aqueous solutions of hydrolyzed Reactive Black 5, hydrolyzed Reactive Blue 19 and hydrolyzed Reactive Red 195, dye adsorption kinetics and the corresponding kinetic equations, and uptake capacity of different hydrolyzed dyes using HTCC/OMMT hybrid, dimensions of the hydrolyzed dyes (PDF)

AUTHOR INFORMATION

Corresponding Authors

*E-mail: R.Menzel@leeds.ac.uk. Phone: +44 (0)113 3436407 (R.M.).

*E-mail: paulmichael@gmail.com. (P.H.)

ORCID

Peng Huang: 0000-0001-6614-7310

Paul Thornton: 0000-0003-3876-1617

Long Lin: 0000-0001-9123-5208

Robert Menzel: 0000-0002-4498-8095

Author Contributions

The experiments were designed by Robert Menzel and Peng Huang, and were performed by Peng Huang. The manuscript was written through contributions of all authors. All authors have given approval to the final version of the manuscript.

Notes

The authors declare no competing financial interest.

ACKNOWLEDGMENTS

The authors would like to thank the University of Leeds and the China Scholarship Council for providing the funding.

REFERENCES

1. Qiu, W.-Z.; Yang, H.-C.; Wan, L.-S.; Xu, Z.-K., Co-deposition of Catechol/Polyethyleneimine on Porous Membranes for Efficient Decolorization of Dye Water. *Journal of Materials Chemistry A* **2015**, *3*, (27), 14438-14444.
2. Ramya, M.; Karthika, M.; Selvakumar, R.; Raj, B.; Ravi, K., A Facile and Efficient Single Step Ball Milling Process for Synthesis of Partially Amorphous Mg-Zn-Ca Alloy Powders for Dye Degradation. *Journal of Alloys and Compounds* **2017**, *696*, 185-192.
3. Kansal, S. K.; Kumari, A., Potential of *M. oleifera* for the Treatment of Water and Wastewater. *Chemical Reviews* **2014**, *114*, (9), 4993-5010.
4. Broadbent, A. D., *Basic Principles of Textile Coloration*. Society of Dyers and Colorists West Yorkshire: 2001; Vol. 132.
5. Ali, I., New Generation Adsorbents for Water Treatment. *Chemical Reviews* **2012**, *112*, (10), 5073-5091.
6. Chacón-Patiño, M. L.; Blanco-Tirado, C.; Hinestroza, J. P.; Combariza, M. Y., Biocomposite of Nanostructured MnO₂ and Figue Fibers for Efficient Dye Degradation. *Green Chemistry* **2013**, *15*, (10), 2920-2928.
7. Zhu, H.-Y.; Jiang, R.; Xiao, L.; Li, W., A Novel Magnetically Separable γ -Fe₂O₃ Crosslinked Chitosan Adsorbent: Preparation, characterization and Adsorption Application for Removal of Hazardous Azo Dye. *Journal of Hazardous Materials* **2010**, *179*, (1), 251-257.
8. Liu, X. D.; Yan, L.; Yin, W. Y.; Zhou, L. J.; Tian, G.; Shi, J. X.; Yang, Z. Y.; Xiao, D. B.; Gu, Z. J.; Zhao, Y. L., A Magnetic Graphene Hybrid Functionalized with Beta-cyclodextrins for Fast and Efficient Removal of Organic Dyes. *Journal of Materials Chemistry A* **2014**, *2*, (31), 12296-12303.
9. Qin, Y.; Wang, L.; Zhao, C.; Chen, D.; Ma, Y.; Yang, W., Ammonium-functionalized Hollow Polymer Particles as a pH-responsive Adsorbent for Selective Removal of Acid Dye. *ACS Applied Materials & Interfaces* **2016**, *8*, (26), 16690-16698.
10. Kim, Y.; Bae, J.; Park, H.; Suh, J.-K.; You, Y.-W.; Choi, H., Adsorption Dynamics of Methyl Violet onto Granulated Mesoporous Carbon: Facile Synthesis and Adsorption Kinetics. *Water Research* **2016**, *101*, 187-194.

11. Karcher, S.; Kornmüller, A.; Jekel, M., Anion Exchange Resins for Removal of Reactive Dyes From Textile Wastewaters. *Water Research* **2002**, *36*, (19), 4717-4724.
12. Martínez-Huitile, C. A.; Rodrigo, M. A.; Sirés, I.; Scialdone, O., Single and Coupled Electrochemical Processes and Reactors for the Abatement of Organic Water Pollutants: A Critical Review. *Chemical Reviews* **2015**, *115*, (24), 13362-13407.
13. Selvam, P. P.; Preethi, S.; Basakaralingam, P.; Thinakaran, N.; Sivasamy, A.; Sivanesan, S., Removal of Rhodamine B from Aqueous Solution by Adsorption onto Sodium Montmorillonite. *Journal of Hazardous Materials* **2008**, *155*, (1), 39-44.
14. Cheng, W.; Ding, C.; Nie, X.; Duan, T.; Ding, R., Fabrication of 3D Macroscopic Graphene Oxide Composites Supported by Montmorillonite for Efficient U(VI) Wastewater Purification. *ACS Sustainable Chemistry & Engineering* **2017**, *5*, (6), 5503-5511.
15. Zhang, H.; Kim, Y. K.; Hunter, T. N.; Brown, A. P.; Lee, J. W.; Harbottle, D., Organically Modified Clay with Potassium Copper Hexacyanoferrate for Enhanced Cs⁺ Adsorption Capacity and Selective Recovery by Flotation. *Journal of Materials Chemistry A* **2017**, *5*, (29), 15130-15143.
16. Teng, C.; Qiao, J.; Wang, J.; Jiang, L.; Zhu, Y., Hierarchical Layered Heterogeneous Graphene-poly (N-isopropylacrylamide)-clay Hydrogels with Superior Modulus, Strength, and Toughness. *ACS Nano* **2015**, *10*, (1), 413-420.
17. Gao, G.; Du, G.; Sun, Y.; Fu, J., Self-healable, Tough, and Ultrastretchable Nanocomposite Hydrogels Based on Reversible Polyacrylamide/Montmorillonite Adsorption. *ACS Applied Materials & Interfaces* **2015**, *7*, (8), 5029-5037.
18. Tedeschi, C.; Caruso, F.; Möhwald, H.; Kirstein, S., Adsorption and Desorption Behavior of an Anionic Pyrene Chromophore in Sequentially Deposited Polyelectrolyte-dye Thin Films. *Journal of the American Chemical Society* **2000**, *122*, (24), 5841-5848.
19. Kim, J.-K.; Kim, D. H.; Joo, S. H.; Choi, B.; Cha, A.; Kim, K. M.; Kwon, T.-H.; Kwak, S. K.; Kang, S. J.; Jin, J., Hierarchical Chitin Fibers with Aligned Nanofibrillar Architectures: A Nonwoven-Mat Separator for Lithium Metal Batteries. *ACS Nano* **2017**, *11*, (6), 6114-6121.
20. Crini, G.; Badot, P.-M., Application of Chitosan, a Natural Aminopolysaccharide, for Dye Removal From Aqueous Solutions by Adsorption Processes using Batch Studies: A Review of Recent Literature. *Progress in Polymer Science* **2008**, *33*, (4), 399-447.
21. Sashiwa, H.; Kawasaki, N.; Nakayama, A.; Muraki, E.; Yamamoto, N.; Aiba, S.-i., Chemical Modification of Chitosan. 14: Synthesis of Water-Soluble Chitosan Derivatives by Simple Acetylation. *Biomacromolecules* **2002**, *3*, (5), 1126-1128.
22. Ryu, S.; Kim, H.; Kang, S.; Shin, K.; Jung, S.-Y.; Heo, J.; Han, J.; Yoon, J.-K.; Lee, J.-R.; Hong, J.; Ahn, K. H.; Hyeon, T.; Hwang, N. S.-Y.; Kim, B.-S., Reversible Cell Layering for Heterogeneous Cell Assembly Mediated by Ionic Cross-Linking of Chitosan and a Functionalized Cell Surface Membrane. *Chemistry of Materials* **2017**, *29*, (12), 5294-5305.
23. Lazaridis, N. K.; Kyzas, G. Z.; Vassiliou, A. A.; Bikiaris, D. N., Chitosan Derivatives as Biosorbents for Basic Dyes. *Langmuir* **2007**, *23*, (14), 7634-7643.
24. Chojnacka, K., Biosorption and Bioaccumulation—the Prospects for Practical Applications. *Environment International* **2010**, *36*, (3), 299.
25. Wang, L.; Wang, A., Adsorption Properties of Congo Red From Aqueous Solution Onto N,O-carboxymethyl-chitosan. *Bioresource Technology* **2008**, *99*, (5), 1403-1408.
26. Zhao, S.-h.; Wu, X.-t.; Guo, W.-c.; Du, Y.-m.; Yu, L.; Tang, J., N-(2-hydroxy)propyl-3-trimethyl Ammonium Chitosan Chloride Nanoparticle as a Novel Delivery System for Parathyroid Hormone-Related Protein 1–34. *International Journal of Pharmaceutics* **2010**, *393*, (1–2), 269-273.
27. Huang, P.; Kazlauciuonas, A.; Menzel, R.; Lin, L., Determining the Mechanism and Efficiency of Industrial Dye Adsorption through Facile Structural Control of Organo-montmorillonite Adsorbents. *ACS Applied Materials & Interfaces* **2017**, *9*, (31), 26383-26391.
28. Nayar, S. B.; Freeman, H. S., Hydrolyzed Reactive Dyes. Part 1: Analyses via Fast Atom Bombardment and Electrospray Mass Spectrometry. *Dyes and Pigments* **2008**, *79*, (2), 89-100.
29. Shaker, A. M.; Komy, Z. R.; Heggy, S. E. M.; El-Sayed, M. E. A., Kinetic Study for Adsorption Humic Acid on Soil Minerals. *The Journal of Physical Chemistry A* **2012**, *116*, (45), 10889-10896.
30. Xue, G.; Gao, M.; Gu, Z.; Luo, Z.; Hu, Z., The Removal of p-nitrophenol From Aqueous Solutions by Adsorption using Gemini Surfactants Modified Montmorillonites. *Chemical Engineering Journal* **2013**, *218*, 223-231.
31. Doğan, M.; Özdemir, Y.; Alkan, M., Adsorption Kinetics and Mechanism of Cationic Methyl Violet and Methylene Blue Dyes onto Sepiolite. *Dyes and Pigments* **2007**, *75*, (3), 701-713.
32. Nandi, B.; Goswami, A.; Purkait, M., Adsorption Characteristics of Brilliant Green Dye on Kaolin. *Journal of Hazardous Materials* **2009**, *161*, (1), 387-395.
33. Broadbent, A. D., Basic Principles of Textile Coloration. **2001**.
34. Gulnaz, O.; Kaya, A.; Dincer, S., The Reuse of Dried Activated Sludge for Adsorption of Reactive Dye. *Journal of Hazardous Materials* **2006**, *134*, (1), 190-196.
35. Hesselink, F. T., On the Theory of Polyelectrolyte Adsorption: The Effect on Adsorption Behavior of the Electrostatic Contribution to the Adsorption Free Energy. *Journal of Colloid and Interface Science* **1977**, *60*, (3), 448-466.
36. Van de Steeg, H. G.; Cohen Stuart, M. A.; De Keizer, A.; Bijsterbosch, B. H., Polyelectrolyte Adsorption: a Subtle Balance of Forces. *Langmuir* **1992**, *8*, (10), 2538-2546.
37. Wu, F.-C.; Tseng, R.-L.; Juang, R.-S., Initial Behavior of Intraparticle Diffusion Model used in the Description of Adsorption Kinetics. *Chemical Engineering Journal* **2009**, *153*, (1), 1-8.

ARTICLE

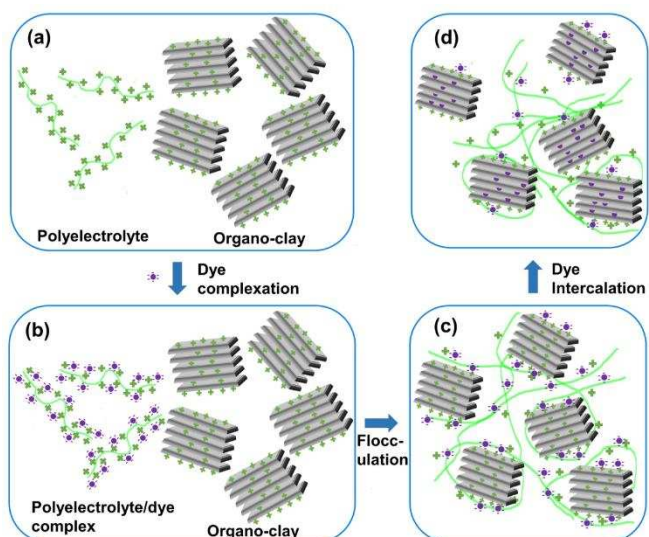


Figure above: Dye-mediated flocculation and sorption in the polyelectrolyte/organo-clay hybrid system, (a) polyelectrolyte/organo-clay hybrid; (b) Dye complexation; (c) Flocculation; (d) Dye intercalation.